



Contents lists available at SciVerse ScienceDirect

Chemical Engineering Journal

journal homepage: www.elsevier.com/locate/cejChemical
Engineering
Journal

A rapid synthesis route for Sn-Beta zeolites by steam-assisted conversion and their catalytic performance in Baeyer–Villiger oxidation

Zihua Kang^a, Xiongfu Zhang^{a,*}, Haiou Liu^a, Jieshan Qiu^a, King Lun Yeung^{b,c}

^a State Key Laboratory of Fine Chemicals, School of Chemical Engineering, Dalian University of Technology, Dalian 116024, PR China

^b Department of Chemical and Biomolecular Engineering, The Hong Kong University of Science and Technology, Clear Water Bay, Kowloon, Hong Kong Special Administrative Region

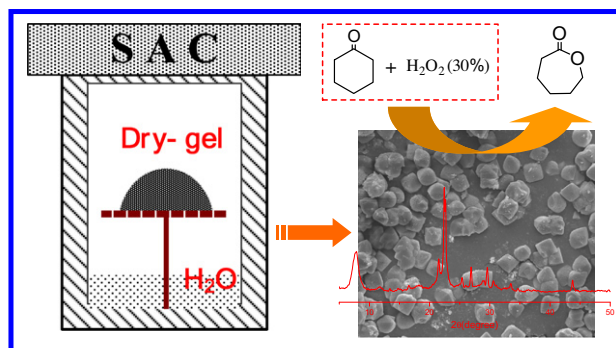
^c Division of Environment, The Hong Kong University of Science and Technology, Clear Water Bay, Kowloon, Hong Kong Special Administrative Region

HIGHLIGHTS

- ▶ A steam-assisted conversion (SAC) method is used to rapidly synthesize Sn-Beta zeolites.
- ▶ Sn-Beta zeolites with high crystallinity and BEA topology could successfully be synthesized by SAC method.
- ▶ The Sn-Beta by SAC method can demonstrate good catalytic activity for cyclohexanone oxidation with 30% H₂O₂.

GRAPHICAL ABSTRACT

A steam-assisted conversion (SAC) method was used to rapidly synthesize Sn-Beta zeolites with high crystallinity and yield. The Sn-Beta zeolites could exhibit good catalytic activity for Baeyer–Villiger (B–V) oxidation reaction of cyclohexanone to ϵ -caprolactone using aqueous H₂O₂ (30%) as oxidant.



ARTICLE INFO

Article history:

Received 26 July 2012

Received in revised form 20 November 2012

Accepted 4 December 2012

Available online xxx

Keywords:

Zeolite

Sn-Beta

Steam-assisted conversion

B–V oxidation

Cyclohexanone

ABSTRACT

Sn-Beta zeolites were prepared by a rapid and clean steam-assisted conversion (SAC) method from dry stannosilicate gel. The amorphous gel was converted to highly crystalline Sn-Beta within 5 h at mild reaction temperature of 453 K. The properties of the as-prepared samples were characterized by XRD, SEM, FT-IR, UV–Vis, UV-Raman, ICP and N₂ adsorption. A high gel conversion to BEA can be obtained with Sn⁴⁺ inserted in the zeolite framework. The SAC method was successfully used to produce pure silica Beta zeolite (Si/Sn = ∞) to Sn-Beta zeolite with 3.8 wt.% SnO₂ (i.e., Si/Sn = 83). The Sn-Beta prepared by SAC method is an efficient catalyst for Baeyer–Villiger (B–V) reaction of cyclohexanone to ϵ -caprolactone.

© 2012 Elsevier B.V. All rights reserved.

1. Introduction

Tin-containing zeolites are of considerable interest due to their unique chemistry and applications [1–4]. The Sn-Beta zeolite

having large 3D pore structure is shown to be very active and chemoselective catalyst for many important organic reactions [5], such as Baeyer–Villiger (B–V) oxidation [6], Meerwein–Ponndorf–Verley (MPV) reduction [7], Oppenauer oxidations [8] as well as sugar conversion to lactic acid derivatives [9], isomerization of glucose to fructose [10] and conversion of carbohydrates to 5-(hydroxymethyl)-furfural (HMF) [11]. The conventional

* Corresponding author. Tel./fax: +86 411 84986155.

E-mail address: xfzhang@dlut.edu.cn (X. Zhang).

preparation of Sn-Beta is via hydrothermal synthesis in fluoride system [6–11]. Seeds are often required and are prepared by dealumination of nano-sized Al-Beta zeolites with concentrated nitric acid. Besides the lengthy synthesis time, the use of hydrofluoric acid as mineralizer produces unwanted pollutions and hazards. Furthermore, it is often difficult to adjust the H_2O/SiO_2 ratio when silicon alkoxides are used as the removal of alcohol also evaporates water that often leads to poor synthesis reproducibility [12–16]. Thus, the process is energy intensive and difficult to scale-up. Recently, Li et al. [17] have reported an alternative route for preparing of Sn-Beta zeolite by a solid–gas reaction of dealuminated Al-Beta zeolite at high temperature. The process although attractive is complex as well as very energy intensive.

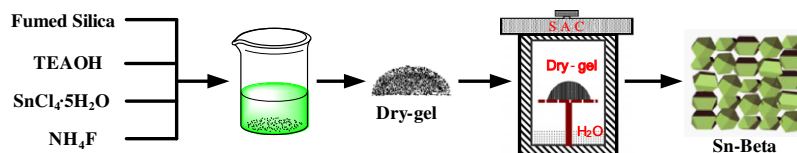
This work explores the possibility of preparing Sn-Beta zeolites by steam-assisted conversion (SAC) method. This method transforms a precursor gel into porous crystalline zeolites [18–20], molecular sieves [21–25] and metal organic frameworks (MOFs) [26] using steam. SAC method is characterized by rapid synthesis [18,27,28] at milder conditions of pH and temperature, while requiring less SDA and thus generating less waste than the conventional hydrothermal synthesis route. There is no prior report on the preparation Sn-Beta by SAC method, and this work aims to investigate the synthesis of active Sn-Beta catalyst for Baeyer–Villiger (B–V) oxidation of cyclohexanone to ϵ -caprolactone.

2. Experimental

2.1. Synthesis

Sn-Beta zeolites were prepared according to Scheme 1. A wet gel was first prepared from fumed silica powder (SiO_2 , 99.8%, Shenyang Chemical Co. Ltd.), $SnCl_4 \cdot 5H_2O$ (98%, Tianjin Kermel Chemical Reagent Co. Ltd.), tetraethylammonium hydroxide (TEAOH, 40%, Zhejiang Kente Chemical Co., Ltd.) and NH_4F (98%, Tianjin Kermel Chemical Reagent Co. Ltd.). Following careful drying at 333 K for 6 h, a dry gel with a composition of 1 SiO_2 : 0.27 (TEA) $_2$: 0.002–0.012 SnO_2 : 0.54 NH_4F : 7.5 H_2O was obtained. The 2 g dry stannosilicate gel was ground into powder and placed in a homemade autoclave that prevents water condensation on the dry gel during the steam-assisted conversion process. This precaution allows reproducible gel composition to be obtained. 1.5 mL water was added to the autoclave and the steam was generated at 453 K. Products were obtained following 3–6 h of treatment and were washed and dried at 383 K for 8 h prior air calcination at 823 K for 6 h to remove the organic template.

Sn-Beta zeolite with Si/Sn = 120 was prepared by conventional method according to the procedure reported by Corma et al. [6]. The synthesis was carried out in a fluoride system using TEOS (98%, Tianjin Kermel Chemical Reagent Co. Ltd.) as



Scheme 1. Illustration of the Sn-Beta zeolite preparation by SAC method.

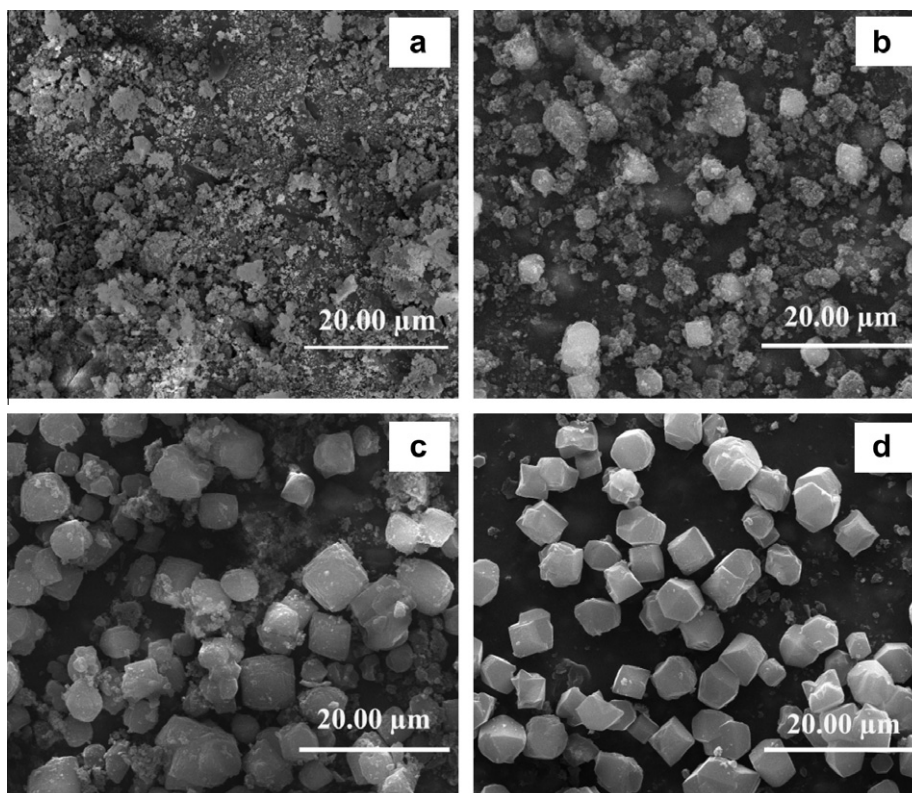


Fig. 1. SEM images of as-synthesized Sn-Beta (125) samples at different crystallization time: (a) 0 h, (b) 2 h, (c) 4 h, and (d) 6 h.

the silica source, $\text{SnCl}_4 \cdot 5\text{H}_2\text{O}$, TEOAH, and HF (48%, Shenyang Chemical Co. Ltd.). The TEOS was hydrolyzed in an aqueous solution of TEOAH with stirring before adding the $\text{SnCl}_4 \cdot 5\text{H}_2\text{O}$ solution. The gel was aged with stirring until all ethanol from the hydrolysis of TEOS had evaporated. HF was then added, resulting in a viscous gel containing 1 SiO_2 : 0.0083 SnO_2 : 0.54 TEOAH: 0.54 HF: 7.5 H_2O . This gel was transferred to a Teflon-lined stainless steel autoclave and heated to 413 K. After 20 days of crystallization, the product was recovered by filtration and thoroughly washed with water before drying overnight at 373 K. The zeolite was then calcined in air at 853 K for 6 h to obtain Sn-Beta-HTS (120) sample.

2.2. Characterization

The Sn-Beta zeolites were examined by X-ray diffraction (XRD), scanning electron microscopy (SEM) and nitrogen physiosorption to obtain the structural and textural data on the zeolites. The chemistry and elemental composition of the Sn-Beta zeolites were determined by UV-Vis, FTIR, UV-Raman and ICP-AES methods. Powder X-ray diffractograms were collected by Philips Analytical X-ray diffractometer using the $\text{Cu K}\alpha$ radiation, operating at 30 kV and 30 mA. The synthesis product powder was examined by scanning electron microscope (FEI Quanta 650) after coating with a thin layer of Au-Pd to prevent sample charging. N_2 physiosorption isotherms were measured by Autosorb-1 (Quantachrome Instruments) at 77 K. Prior to the measurements, the sample was degassed at 473 K for at least 6 h. Fourier-transform infra-red spectra (FT-IR) of the product were taken on a Nicolet-5DX spectrometer at room-temperature. The samples were ground with KBr powder, pressed into thin wafers and dried at 393 K for 1 h in air before analysis. The diffuse reflectance UV-Vis spectra were recorded in the range 200–600 nm in a Shimadzu V-550 spectrometer using BaSO_4 as reference standard. UV-Raman spectra were recorded on a DL-2 Raman spectrometer. A 244-nm laser line of LEXEL LASER (95-SHG) was used as the excitation source. Acton triple monochromator was used as the spectrometer for Raman scattering. The spectra were collected by a Princeton CCD detector. The elemental composition of the samples was analyzed by using inductively-coupled plasma, atomic emission spectrometer (ICP-AES, Optima 2000DV).

2.3. Baeyer–Villiger (B–V) oxidation reaction

The Baeyer–Villiger oxidation of cyclohexanone to ϵ -caprolactone using H_2O_2 as liquid oxidant was performed in a round-bottom flask (50 mL) fitted with a condenser and a magnetic stirrer. 1.08 g cyclohexanone (>99.5%, Tianjin Kermel Chemical Reagent Co. Ltd.) dissolved in 30.0 g dioxane (>99.5%, Tianjin Kermel Chemical Reagent Co. Ltd.) was reacted with 1.59 g hydrogen peroxide (30% Sinopharm Chemical Reagent Co. Ltd.) using 0.5 g catalyst at a reaction temperature of 363 K. The temperature was maintained by a recirculating water bath and reflux unit, and metered amount of the reaction mixture were obtained at regular intervals for analysis by gas chromatograph, a GC7890F from Shanghai Techcomp Ltd. The gas chromatograph was equipped with a capillary column (HP-5 column, 15 m \times \varnothing 0.32 mm \times 0.5 μm) and a flame ionization detector. A study of catalyst recovery and regeneration was carried out for the Sn-Beta(125) sample. The catalyst was washed 2 times with dioxane (catalyst/dioxane = 1:30 g g^{-1}) after each run, and put into a new reaction solution. The recovered catalyst was dried and re-calcined at 823 K for 6 h under air before its reuse in subsequent catalytic runs.

3. Results and discussion

3.1. Sn-Beta zeolite by SAC method

Fig. 1 shows the transformation of stannosilicate gel to Sn-Beta zeolites during steam-assisted crystallization process. Crystalline solids with regular facets (Fig. 1b) are crystallized from the amorphous gel (Fig. 1a) after 2 h of steam reaction. The amorphous phase disappeared after 4 h into the reaction and complete transformation of the amorphous gel particles into crystalline zeolite crystals is observed after 6 h.

Powder X-ray diffraction in Fig. 2a shows that the initial dry gel (amorphous) is completely transformed into Sn-Beta in 6 h by SAC method at the reaction temperature of 453 K. The Sn-Beta(125) sample (Note: 125 represents feed $\text{SiO}_2/\text{SnO}_2 = 125$ in dry gel) displays typical BEA diffraction pattern [6,29,30]. Only Sn-Beta zeolite is formed and no other crystalline phases such as SnO_2 are observed. This suggests that SAC method can produce Sn-Beta zeolite of high purity and crystallinity. The absence of amorphous phase in SEM and PXRD indicates that the gels were complete transformed into the uniform-sized Sn-Beta zeolites ($6 \pm 1 \mu\text{m}$). The nitrogen adsorption–desorption isotherms of Sn-Beta(125) in Fig. 2b is mainly that of microporous zeolites, but for a slight hysteresis loop that could arise from the aggregation of the zeolite nanocrystals [31,32]. Indeed a bimodal distribution can be observed from this sample with the main pore size centered at around 0.56 nm.

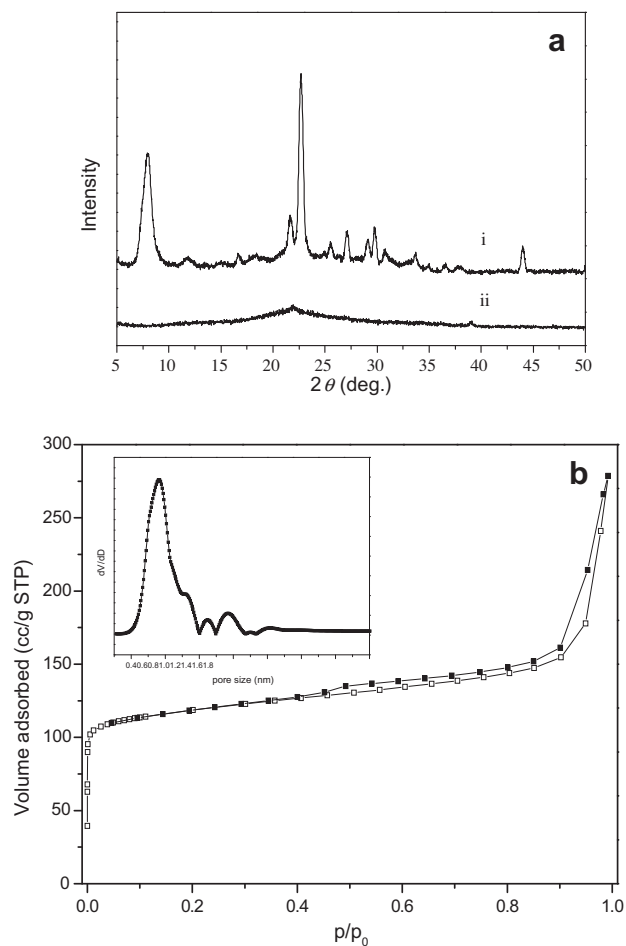


Fig. 2. (a) XRD patterns of (i) Sn-Beta (125), (ii) dry gel; (b) N_2 sorption isotherms of Sn-Beta (125) zeolite (The insert provides the micropore pore size distribution (HK method) of the Sn-Beta zeolite with sharp peak at 0.56 nm).

There is general consensus that the isolated Sn(IV) atoms in the Sn-Beta zeolite framework are responsible for its excellent catalytic activity and selectivity for selective oxidation reactions. The IR band at ca. 960 cm^{-1} in the FT-IR spectrum is often taken as an indication of tin substitution into the zeolite framework [33–35]. The FTIR spectrum of Sn-Beta(125) in Fig. 3a displays an absorption band at ca. 960 cm^{-1} (cf. Fig. 3a-(ii)) that is absent in the pure silica Si-Beta (Fig. 3a-(i)). Similarly, only Sn-Beta(125) shows an absorption band in UV-Vis spectra (Fig. 3b-(iii)) at the wavelength region of 210–220 nm originating from the isolated Sn atoms in the zeolite framework [33]. The SnO_2 (Fig. 3b-(i)) and calcined dry gel (Fig. 3b-(ii)) have a broad absorbance at ca. 250–280 nm assigned to extra-framework Sn species and/or SnO_2 crystal phases [34]. This means that there are no extra-framework tin species in Sn-Beta(125) prepared by SAC method. UV Raman spectroscopy has high sensitivity for transition metals in zeolite framework [36] and can detect very small amounts of these metals in zeolites. Fig. 3c shows the UV Raman spectra of SnO_2 , Si-Beta and Sn-Beta using a 244 nm light source that is close in energy to the charge transfer band of Sn-Beta at 210 nm. Characteristic bands at $324, 344, 400, 428, 468$ and 825 cm^{-1} belonging to zeolite Beta are observed in both Sn-Beta(125) (Fig. 3c-(ii)) and Si-Beta (Fig. 3c-(iii)) samples [22,37]. The strong Raman band at 705 cm^{-1} is found in Sn-Beta(125) and not in Si-Beta and is attributed to the substitution of tin atoms for silicon in the zeolite framework. The SnO_2 phase is not observed in the Raman spectrum

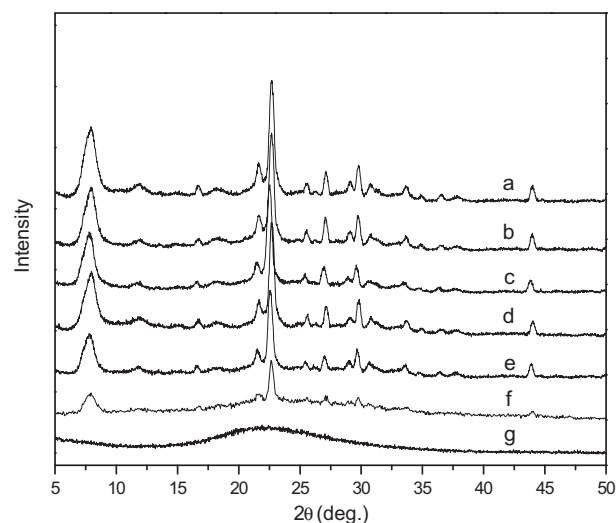


Fig. 4. XRD patterns of the Sn-Beta samples with different $\text{SiO}_2/\text{SnO}_2$ ratios: (a) Si-Beta, (b) 500, (c) 250, (d) 125, (e) 100, (f) 83 and (g) 75.

of the Sn-Beta(125) prepared by SAC method despite having a high Sn loading of 3.81 wt.% SnO_2 . This suggests that, at least up to the detection limit of Raman spectroscopy, the samples do not appear to have extra-framework SnO_2 .

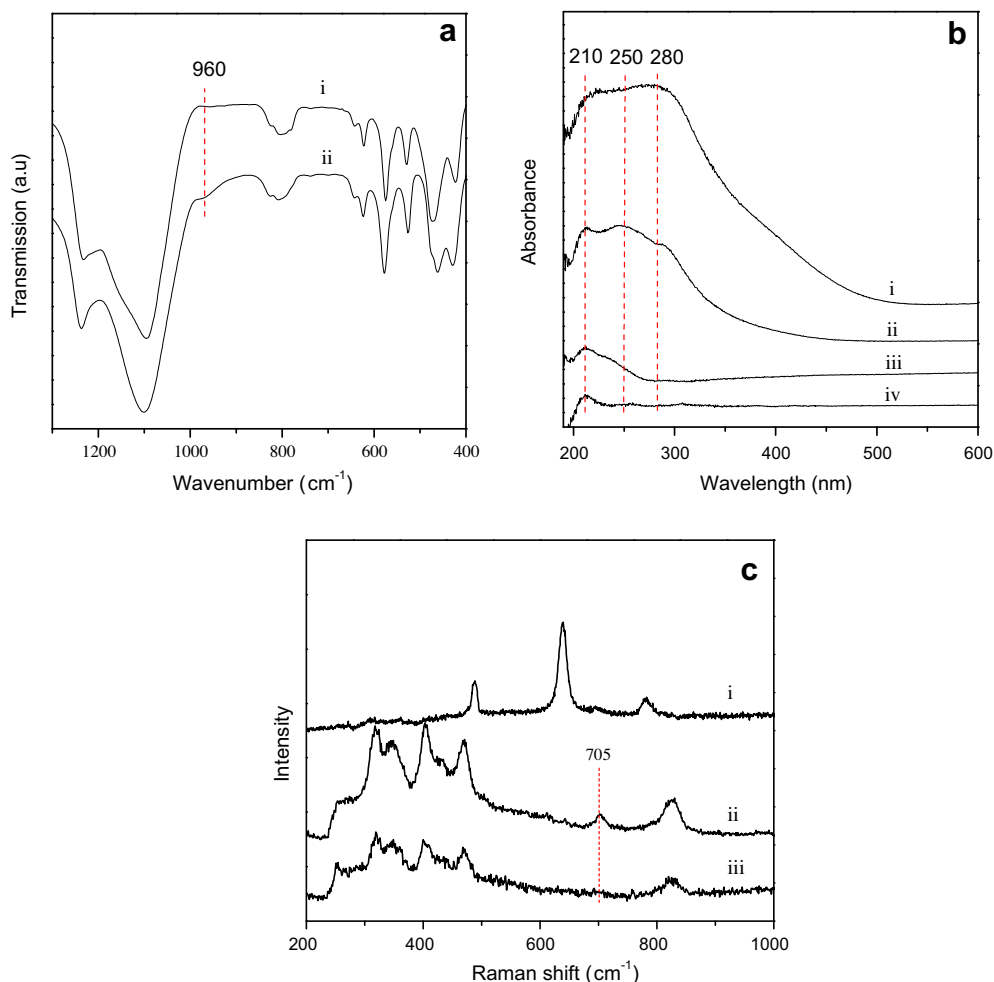


Fig. 3. (a) FT-IR spectra of (i) Si-Beta, (ii) Sn-Beta(125); (b) UV-Vis spectra of (i) SnO_2 , (ii) calcined dry-gel powder, (iii) Sn-Beta(125), (iv) Si-Beta; (c) UV Raman spectra of (i) SnO_2 , (ii) Sn-Beta(125), (iii) Si-Beta.

Table 1
Properties of the Sn-Beta samples obtained by SAC method.

Sample	Time	Structure ^a	SiO ₂ /SnO ₂ ratio		BET surface area ^c (m ² g ⁻¹)	PV ^d (ml g ⁻¹)
			Dry gel	Product ^b		
Si-Beta	3 h	BEA (100)	∞	∞	500.5	0.208
Sn-Beta(500) ^e	3 h	BEA (95.7)	500	490.1	475.4	0.188
Sn-Beta(250)	4 h	BEA (93.2)	250	189.2	453.4	0.187
Sn-Beta(125)	5 h	BEA (82.6)	125	93.0	440.0	0.157
Sn-Beta(100)	24 h	BEA (77.5)	100	80.0	421.6	0.147
Sn-Beta(83)	60 h	BEA (69.6)	83	64.1	303.7	0.116
Sn-Beta(75)	200 h	Amorphous	75	75.0	–	–
Sn-Beta-HTS(120) ^f	20 days	BEA (86.7)	120	128.1	467.0	0.203

^a XRD analysis. The number in the parentheses indicates the relative crystallinity.

^b Determined by ICP.

^c Specific surface area given by N₂ adsorption at 77 K.

^d PV, micropore volume.

^e Sn-Beta(500) represents feed SiO₂/SnO₂ mole ratio = 500.

^f Prepared by conventional hydrothermal synthesis at 413 K for 20 days (feed SiO₂/SnO₂ = 120).

3.2. Catalytic Sn-Beta zeolite

The catalytic properties of metallosilicates depend on the concentration and coordination of heteroatoms within the zeolite structure and the degree of isomorphous substitution is dictated by the zeolite topology, heteroatom chemistry and synthesis

methodology [38–41]. Thus, it is important to examine the preparation of Sn-Beta zeolites with varying amount of Sn loading by SAC method. Stannosilicate dry gels containing different amount of SnO₂ were prepared and transformed by SAC method. The PXRD patterns in Fig. 4 shows that all the Sn-Beta zeolites with SiO₂/SnO₂ ratios ≥ 83 display only the characteristic diffraction peaks of BEA.

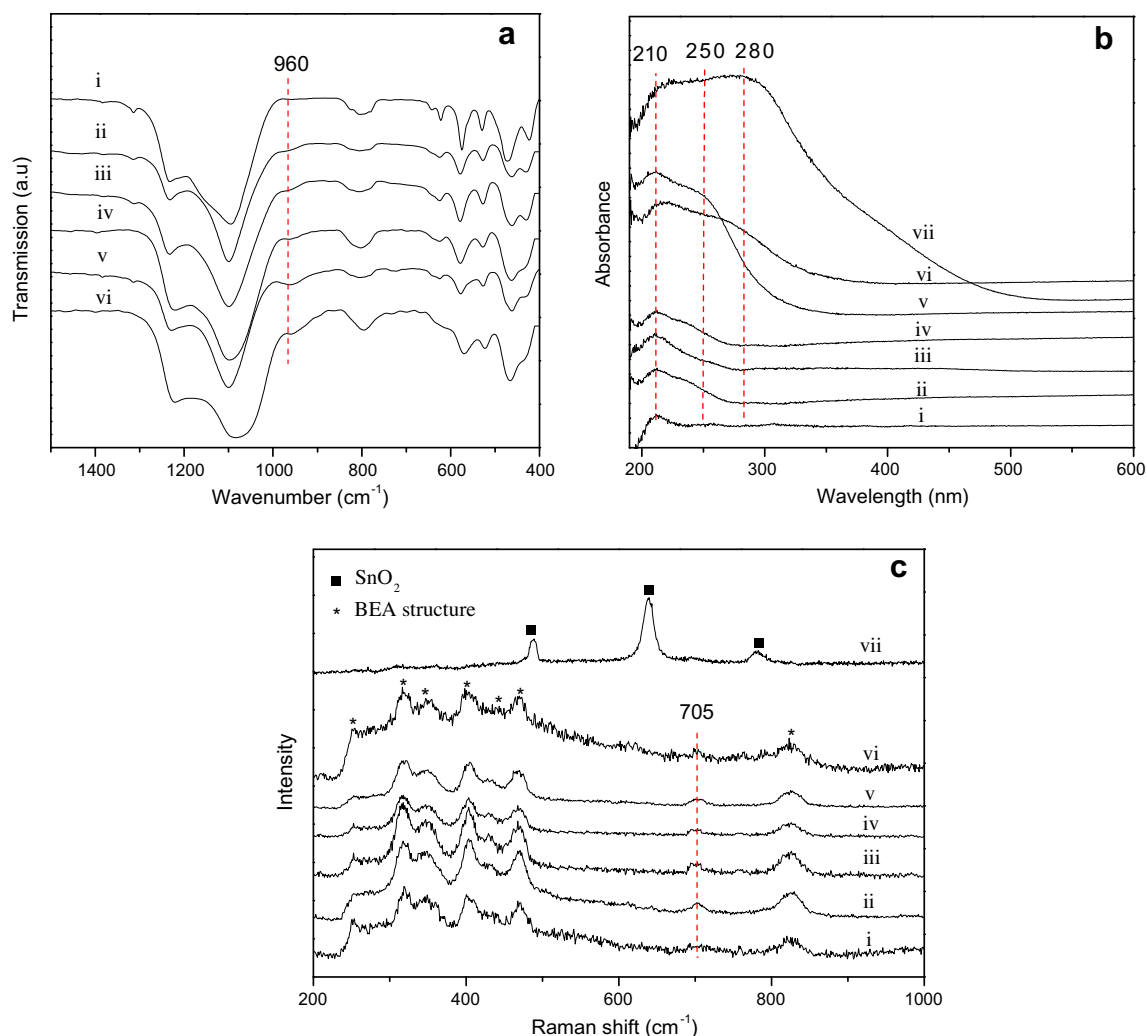


Fig. 5. (a) FT-IR spectra of (i) Si-Beta, (ii) Sn-Beta(500), (iii) Sn-Beta(250), (iv) Sn-Beta(125), (v) Sn-Beta(100) and (vi) Sn-Beta(83); (b) UV-Vis and (c) UV Raman spectra of the Sn-Beta samples with different SiO₂/SnO₂ ratios: (i) Si-Beta, (ii) 500, (iii) 250, (iv) 125, (v) 100, (vi) 83 and (vii) SnO₂.

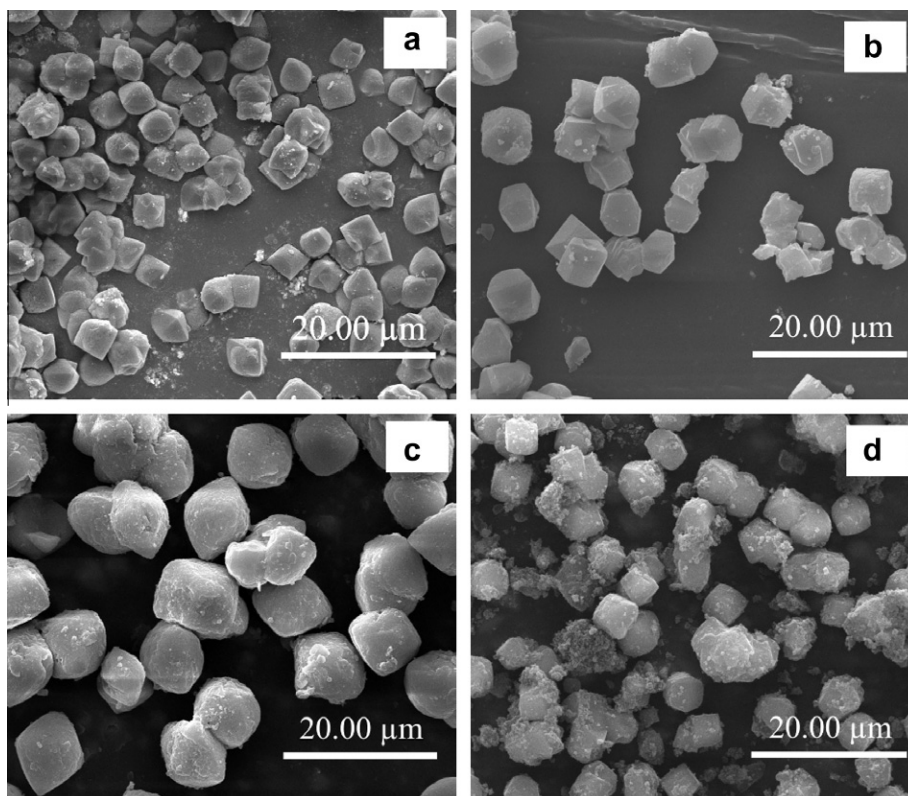


Fig. 6. SEM images of the Sn-Beta samples with different $\text{SiO}_2/\text{SnO}_2$ ratios: (a) 500, (b) 250, (c) 125 and (d) 100.

Table 2
Catalytic properties of the Sn-Beta samples obtained by SAC method^a.

Entry	Catalyst	Tin content (SnO_2 wt.%) ^b	Cyclohexanone conv (%) ^c	Lactone sel (%) ^d
1	Si-Beta	0.00	0.0	0.00
2	Sn-Beta(500)	0.51	17.1	98.85
3	Sn-Beta(250)	1.31	24.8	98.01
4	Sn-Beta(125)	2.63	27.9	99.74
5	Sn-Beta(100)	3.06	36.1	99.48
6	Sn-Beta(83)	3.81	23.6	99.01
8	Sn-Beta-HTS(120)	1.91	32.3	99.95

^a Reaction conditions: Cat., 500 mg; cyclohexanone, 10 mmol; H_2O_2 (30 wt.%), 15 mmol; dioxane, 30 mL; temp, 363 K; time, 3 h.

^b Determined by ICP-AES.

^c Conversion = (moles of ketone converted)/(initial moles of ketone) \times 100.

^d Selectivity = (moles of product)/(moles of ketone reacted) \times .

Increasing tin loading slows the crystallization process and lead to lower crystallinity (Table 1). It is not possible to convert stannosilicate dry gel with $\text{SiO}_2/\text{SnO}_2$ ratios ≤ 75 into Sn-Beta even after 200 h of crystallization (Fig. 4g). Comparing the crystallinity of Sn-Beta zeolites to Si-Beta sample (100% crystallinity), Sn-Beta(500), Sn-Beta(250), Sn-Beta(125), Sn-Beta(100) and Sn-Beta(83) have relative crystallinity to Si-Beta of 96%, 93%, 83%, 78% and 70%, respectively. Similar observations were made during substitution Ti in MFI zeolite framework wherein there appears a maximum to the amount of titanium that can be substituted into the zeolite framework regardless of the synthesis route [42,43]. Table 1 summarizes the crystallinity and textural properties (i.e., specific BET surface area and average pore volume) of the Sn-Beta zeolites. The table also lists the $\text{SiO}_2/\text{SnO}_2$ ratio in the stannosilicate dry gel and the actual $\text{SiO}_2/\text{SnO}_2$ ratio in the crystallized Sn-Beta according to ICP-AES analysis. The SnO_2 content of the zeolite increases with the SnO_2 content of the dry gel.

The FTIR, UV-Vis and UV Raman spectra of the Sn-Beta zeolites prepared by SAC method are plotted in Fig. 5. All Sn-Beta zeolites

display an IR absorption band at ca. 960 cm^{-1} that is absent in the pure silica Si-Beta (i), indicating that Sn are mostly incorporated into the zeolite framework (Fig. 5a). The intensity of the band increases with Sn substitution. Fig. 5b shows that all the Sn-Beta zeolites have an absorption band at 210–220 nm in their UV-Vis spectra. The 210 nm band is from the charge transfer from O^{2-} to the tetrahedral coordinated Sn^{4+} dispersed in the zeolite framework, and is a characteristic of Sn-substituted molecular sieves [44]. The intensity of this band increases with higher tin loading. SnO_2 has a broad absorption band in 250–280 nm region as shown in Fig. 5b-(vii). A weak band in 260 nm region is observed in Sn-Beta(83) sample (Fig. 5b-(vi)), the shoulder at 260 nm probably corresponds to partially polymerized hexa-coordinated Sn-O-Sn species. This conjecture can be well supported by the similar band observed in the Ti-containing zeolites[45–47]. The UV Raman spectra of the Sn-Beta zeolites in Fig. 6c display bands associated to the four- (468 cm^{-1}), five- (324 and 344 cm^{-1}), six-membered rings (400 and 428 cm^{-1}) of the BEA zeolite lattice [22]. Except for Si-Beta (i), all the SAC-crystallized Sn-Beta zeolite has an absorption

band at ca. 705 cm^{-1} for Sn substituted in the zeolite lattice. The characteristic bands of SnO_2 are not observed even for the Sn-Beta(83) sample indicating that at least up to the detection limit of UV Raman, there is no significant amount of extra-framework SnO_2 in Sn-Beta zeolites prepared by SAC method. All the Sn-Beta samples have shown only modes of a fully condensed lattice that are assigned to five-membered rings (324 and 344 cm^{-1}), six-membered rings (400 and 428 cm^{-1}), and four membered rings (468 cm^{-1}), indicating that all the samples have BEA structure [22,36]. However, all the crystallized sample has an absorption band at ca. 705 cm^{-1} that is absent in the pure silica Si-Beta (a), which may be caused by most Sn species are incorporated into the zeolite framework.

Tin substitution in the zeolite lattice affects the crystallization rate of Sn-Beta zeolite with the stannosilicate dry gels containing more Sn being more difficult to crystallize and consequently having more amorphous phase and smaller zeolites as products as shown in Fig. 6. Similar observation is made for the synthesis of other metal-substituted zeolites [31,33,35]. However, SAC-method has the advantage over conventional fluoride synthesis method for Sn-Beta zeolites in that pure phase Sn-Beta zeolites having higher SnO_2 loading can be obtained at significantly shorter preparation time. Complete conversion can be obtained with near zero waste generation at significantly less energy expenditure.

3.3. Baeyer–Villiger (B–V) oxidation reaction

The Sn-Beta zeolites prepared by SAC method and the Sn-Beta-HTS(120) prepared by the conventional route were used as catalyst for the Baeyer–Villiger (B–V) oxidation of cyclohexanone with aqueous H_2O_2 (30 wt.%) to ϵ -caprolactone. Table 2 summarizes the results of the reaction study over a reaction time of 3 h. Si-Beta is inactive for the reaction and the catalytic activity of Sn-Beta zeolites increases with Sn content.

The lower conversion of Sn-Beta(83) could be due to the presence of polymerized hexa-coordinated Sn–O–Sn species from the UV–Vis spectrum, but is more likely due to poorer crystallinity. The amorphous phase present in the sample could also block access to the active sites within the zeolitic pores. Indeed, Sn-Beta(83) displays the lowest BET surface area and pore volume among the Sn-Beta zeolites prepared by SAC method. All Sn-Beta catalysts are more than 98% selective for ϵ -caprolactone. These results confirmed that SAC method can prepare Sn-Beta containing highly dispersed Sn species substituted within the zeolite framework. Sn-Beta-HTS(120) prepared by conventional route has higher tin loading, surface area and pore volume, and better catalytic activity compared to Sn-Beta(125) and Sn-Beta(250) prepared by SAC method. The highest conversion was obtained from Sn-Beta(100) prepared by SAC method with SnO_2 content of 3.1 wt.%.

Catalyst deactivation and regeneration were investigated for Sn-Beta(125) prepared by SAC method as shown in Fig. 7. The catalyst was used to catalyze B–V oxidation of cyclohexanone at 363 K with each reaction run lasting 12 h. The catalyst was recovered after each run, washed with the solvent and reused immediately in the next reaction run. Progressive decrease in reaction conversion is observed after each reaction run. At the end of run 4, a reaction conversion of 37% was obtained compared to 49% in run 1. Although catalyst lost between runs is unavoidable, it is estimated to account for only 5% drop in the reaction conversion. Sn-Beta(125) was then recovered, washed and calcined in air at 823 K. The last step is to remove any strong adsorbed organics from the zeolite pores. Elemental analysis indicates that Sn content and textural properties of the Sn-Beta(125) remained unchanged. A conversion of 42% was obtained from the regenerated catalyst.

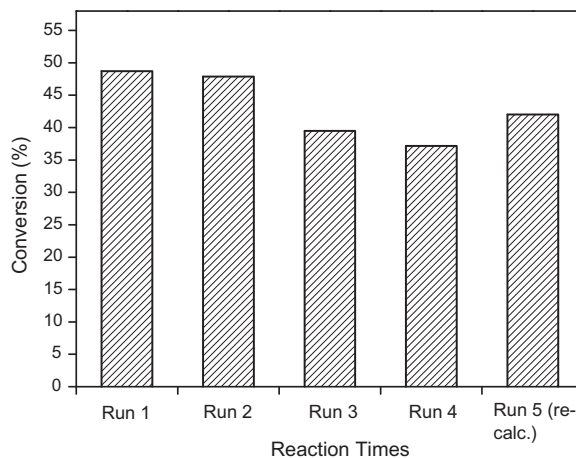


Fig. 7. Recycling test of the Sn-Beta(125) catalyst.

4. Conclusions

In summary, Sn-Beta zeolites of both high crystallinity and yield have been successfully synthesized by a simple steam-assisted conversion method. The prepared Sn-Beta zeolites are active and selective for Baeyer–Villiger (B–V) reaction of cyclohexanone to ϵ -caprolactone. The SAC method is not only faster and more convenient, but also cleaner and less energy intensive than the conventional method. Furthermore, it is possible to prepared Sn-Beta with higher Sn loading using SAC method. Sn-Beta zeolites prepared by SAC have higher Sn-dispersion and substitute in the zeolite lattice. This facile, rapid and efficient synthesis method is expected to provide an economical and scaleable for the industrial application of Sn-Beta zeolite large scale production. Furthermore, this method could provide an alternative route for shaping zeolites for applications in membranes and micro chemical systems [48–52].

Acknowledgements

We gratefully acknowledge the financial supports by National Natural Science Foundation of China (No. 21036006), Universities Science & Research Project of Liaoning Province Education Department (No. 2009S019) and Program for Liaoning Excellent Talents in University (No. LR201008).

References

- [1] M.R. Bryce, Recent progress on conducting organic charge-transfer salts, *Chem. Soc. Rev.* 20 (1991) 355–390.
- [2] N.K. Mal, A.V. Ramaswamy, Oxidation of ethylbenzene over Ti-, V- and Sn-containing silicalites with MFI structure, *Appl. Catal.* 143 (1996) 75–85.
- [3] A. Corma, S. Iborra, A. Velty, Chemical routes for the transformation of biomass into chemicals, *Chem. Rev.* 107 (2007) 2411–2502.
- [4] P.S. Niphadkar, M.S. Kotwa, S.S. Deshpande, V.V. Bokade, P.N. Joshi, Tin-silicalite-1: synthesis by dry gel conversion, characterization and catalytic performance in phenol hydroxylation reaction, *Mater Chem Phys* 114 (2009) 344–349.
- [5] N.K. Mal, A.V. Ramaswamy, Synthesis and catalytic properties of large-pore Sn-beta and Al-free Sn-beta molecular sieves, *Chem. Commun* (1997) 425–426.
- [6] A. Corma, L.T. Nemeth, M. Renz, S. Valencia, Sn-zeolite beta as a heterogeneous chemoselective catalyst for Baeyer–Villiger oxidations, *Nature* 412 (2001) 423–425.
- [7] A. Corma, M.E. Domine, S. Valencia, Water-resistant solid Lewis acid catalysts: Meerwein–Ponndorf–Verley and Oppenauer reactions catalyzed by tin-beta zeolite, *J. Catal.* 215 (2003) 294–304.
- [8] A. Corma, M.E. Domine, L. Nemeth, S. Valencia, Al-free sn-beta zeolite as a catalyst for the selective reduction of carbonyl compounds (Meerwein–Ponndorf–Verley Reaction), *J. Am. Chem. Soc.* 124 (2002) 3194–3195.
- [9] M.S. Holm, S. Saravanamurugan, E. Taarning, Conversion of sugars to lactic acid derivatives using heterogeneous zeotype catalysts, *Science* 328 (2010) 602–605.

- [10] M. Moliner, Y. Román-Leshkov, M.E. Davis, Tin-containing zeolites are highly active catalysts for the isomerization of glucose in water, *Proc. Natl. Acad. Sci. USA* 107 (2010) 6164–6168.
- [11] E. Nikolla, Y. Román-Leshkov, M. Moliner, M.E. Davis, One-Pot synthesis of 5-(Hydroxymethyl)furfural from carbohydrates using tin-Beta zeolite, *ACS Catal.* 1 (2011) 408–410.
- [12] V. Sebastián, I. Díaz, C. Téllez, J. Coronas, J. Santamaría, Spheres of microporous titanosilicate umbite with hierarchical pore systems, *Adv. Funct. Mater.* 18 (2008) 1314–1320.
- [13] L.I. Devriese, J.A. Martens, J.W. Thybaut, G.B. Marin, G.V. Baron, J.F.M. Denayer, A new methodology to probe shape selectivity in porous adsorbents, *Micropor. Mesopor. Mater.* 116 (2008) 607–613.
- [14] J.W. Thybaut, M. Saeyns, G.B. Marin, Hydrogenation kinetics of toluene on Pt/ZSM-22, *Chem. Eng. J.* 90 (2002) 117–129.
- [15] X. Wang, X. Zhang, Y. Wang, H. Liu, J. Qiu, J. Wang, W. Han, K.L. Yeung, Investigating the role of zeolite nanocrystal seeds in the synthesis of mesoporous catalysts with zeolite wall structure, *Chem. Mater.* 23 (2011) 4469–4479.
- [16] X. Zhang, H. Liu, K.L. Yeung, Influence of seed size on the formation and microstructure of zeolite silicalite-1 membranes by seeded growth, *Mater. Chem. Phys.* 96 (2006) 42–50.
- [17] P. Li, G. Liu, H. Wu, Y. Liu, J. Jiang, P. Wu, Postsynthesis and selective oxidation properties of nanosized Sn-Beta zeolite, *J. Phys. Chem. C* 115 (2011) 3663–3670.
- [18] W. Xu, J. Dong, J. Li, J. Li, F. Wu, A novel method for the preparation of zeolite ZSM-5, *J. Chem. Soc. Chem. Commun.* (1990) 755–756.
- [19] R. Cai, Y. Liu, S. Gu, Y. Yan, Ambient pressure dry-gel conversion method for zeolite mfi synthesis using ionic liquid and microwave heating, *J. Am. Chem. Soc.* 132 (2010) 12776–12777.
- [20] R. Chal, C. Gérardin, M. Bulut, S. van Donk, Overview and industrial assessment of synthesis strategies towards zeolites with mesopores, *ChemCatChem* 3 (2011) 67–81.
- [21] J. Zhou, Z. Hua, J. Shi, Q. He, L. Guo, M. Ruan, Synthesis of a hierarchical micro/mesoporous structure by steam-assisted post-crystallization, *Chem. Eur. J.* 15 (2009) 12949–12954.
- [22] K. Möller, B. Yilmaz, R.M. Jacobinas, U. Müller, T. Bein, One-step synthesis of hierarchical zeolite beta via network formation of uniform nanocrystals, *J. Am. Chem. Soc.* 133 (2011) 5284–5295.
- [23] X.B. Ke, L. Xu, C.F. Zeng, L.X. Zhang, N.P. Xu, Synthesis of mesoporous TS-1 by hydrothermal and steam-assisted dry gel conversion techniques with the aid of triethanolamine, *Micropor. Mesopor. Mater.* 106 (2007) 68–75.
- [24] C.M. Song, Y. Feng, L.L. Ma, Characterization and hydroisomerization performance of SAPO-11 molecular sieves synthesized by dry gel conversion, *Micropor. Mesopor. Mater.* 147 (2012) 205–211.
- [25] B. Chen, Y. Huang, Formation of microporous material AlPO₄-18 under dry-gel conversion conditions, *Micropor. Mesopor. Mater.* 143 (2011) 14–21.
- [26] Q. Shi, Z.F. Chen, Z.W. Song, J.P. Li, J.X. Dong, Synthesis of ZIF-8 and ZIF-67 by steam-assisted conversion and an investigation of their tribological behaviors, *Angew. Chem. Int. Ed.* 50 (2011) 672–675.
- [27] A. Sakthivel, A. Iida, K. Komura, Y. Sugi, K.V.R. Chary, Nanosized β -zeolites with tunable particle sizes: Synthesis by the dry gel conversion (DGC) method in the presence of surfactants, characterization and catalytic properties, *Micropor. Mesopor. Mater.* 119 (2009) 322–330.
- [28] T. Tatsumi, N. Jappara, Properties of Ti-beta zeolites synthesized by dry-gel conversion and hydrothermal methods, *J. Phys. Chem. B* 102 (1998) 7126–7131.
- [29] S.M. Maier, A. Jentys, J.A. Lercher, Steaming of zeolite BEA and its effect on acidity: a comparative NMR and IR spectroscopic study, *J. Phys. Chem. C* 115 (2011) 8005–8013.
- [30] R. Hajjar, Y. Millot, P.P. Man, M. Che, S. Dzwigaj, Two kinds of framework al sites studied in BEA zeolite by X-ray diffraction, fourier transform infrared spectroscopy, NMR techniques, and UV Probe, *J. Phys. Chem. C* 112 (2008) 20167–20175.
- [31] R. van Grieken, C. Martos, M. Sanchez-Sanchez, D.P. Serrano, J.A. Melero, J. Iglesias, A.G. Cubero, Synthesis of Sn-silicalite from hydrothermal conversion of SiO₂-SnO₂ xerogels, *Micropor. Mesopor. Mater.* 119 (2009) 176–185.
- [32] X. Wang, X. Zhang, Y. Wang, H. Liu, J. Qiu, J. Wang, W. Han, K.L. Yeung, Performance of TS-1-coated structured packing materials for styrene oxidation reaction, *ACS Catal.* 1 (2011) 437–445.
- [33] M. Sanchez-Sanchez, R. van Grieken, D.P. Serrano, J.A. Melero, On the Sn(II) and Sn(IV) incorporation into the AFI-structured AlPO₄-based framework: the first significantly acidic SnAPO-5, *J. Mater. Chem.* 19 (2009) 6833–6841.
- [34] L.T.Y. Au, J.L.H. Chau, C. Tellez, K.L. Yeung, Preparation of supported Sil-1, TS-1 and VS-1 membranes: Effects of Ti and V metal ions on the membrane synthesis and permeation properties, *J. Membr. Sci.* 183 (2001) 269–291.
- [35] N. Garcia Vargas, S. Stevenson, D.F. Shantz, Synthesis and characterization of tin(IV) MFI: sodium inhibits the synthesis of phase pure materials, *Micropor. Mesopor. Mater.* 152 (2012) 37–49.
- [36] X. Wang, X. Zhang, Y. Wang, H. Liu, J. Wang, J. Qiu, H.L. Ho, W. Han, K.L. Yeung, Preparation and performance of TS-1/SiO₂ egg-shell catalysts, *Chem. Eng. J.* 175 (2011) 408–416.
- [37] B. Mihailova, V. Valtchev, S. Mintova, A.C. Faust, N. Petkov, T. Bein, Interlayer stacking disorder in zeolite beta family: a Raman spectroscopic study, *Phys. Chem. Chem. Phys.* 7 (2005) 2756–2763.
- [38] W. Wang, G. Li, W. Li, L. Liu, Synthesis of hierarchical TS-1 by caramel templating, *Chem. Commun.* 47 (2011) 3529–3531.
- [39] F. Taborda, Z. Wang, T. Willhammar, C. Montes, X. Zou, Synthesis of Al-Si-beta and Ti-Si-beta by the aging-drying method, *Micropor. Mesopor. Mater.* 150 (2012) 38–46.
- [40] J. Dwyer, K. Karim, The incorporation of heteroatoms into faujastic framework by secondary synthesis using aqueous fluoride complexes, *J. Chem. Soc., Chem. Commun.* (1991) 905–906.
- [41] J. Li, J. Yu, R. Xu, Progress in heteroatom-containing aluminophosphate molecular sieves, *Proceedings of the Royal Society A: Mathematical, Physical and Engineering Science* 468 (2012) 1955–1967.
- [42] F. Qiu, X. Wang, X. Zhang, H. Liu, S. Liu, K.L. Yeung, Preparation and properties of TS-1 zeolite and film using Sil-1 nanoparticles as seeds, *Chem. Eng. J.* 147 (2009) 316–322.
- [43] H. Xin, J. Zhao, S. Xu, J. Li, W. Zhang, X. Guo, E.J.M. Hensen, Q. Yang, C. Li, Enhanced catalytic oxidation by hierarchically structured TS-1 zeolite, *J. Phys. Chem. C* 114 (2010) 6553–6559.
- [44] P.S. Niphadkar, A.C. Garade, R.K. Jha, C.V. Rode, P.N. Joshi, Micro-/meso-porous stannosilicate composites (Sn-MFI/MCM-41) via two-step crystallization process: process parameter–phase relationship, *Micropor. Mesopor. Mater.* 136 (2010) 115–125.
- [45] K. Lin, P.P. Pescarmona, H. Vandepitte, D. Liang, G. Van Tendeloo, P.A. Jacobs, Synthesis and catalytic activity of Ti-MCM-41 nanoparticles with highly active titanium sites, *J. Catal.* 254 (2008) 64–70.
- [46] K. Lin, O.I. Lebedev, G. Van Tendeloo, P.A. Jacobs, P.P. Pescarmona, Titanosilicate beads with hierarchical porosity: synthesis and application as epoxidation catalysts, *Chem. Eur. J.* 16 (2010) 13509–13518.
- [47] W. Wang, M. Song, Photocatalytic activity of titania-containing mesoporous SBA-15 silica, *Micropor. Mesopor. Mater.* 96 (2006) 255–261.
- [48] J.L.H. Chau, A.Y.L. Leung, K.L. Yeung, Zeolite micromembranes, *Lab-on-a-Chip* 3 (2003) 53–55.
- [49] K.L. Yeung, X.F. Zhang, W.N. Lau, R. Martin-Aranda, Experiments and modeling of membrane microreactors, *Catal. Today* 110 (2005) 26–37.
- [50] X.B. Wang, X.F. Zhang, H.O. Liu, K.L. Yeung, J.Q. Wang, Preparation of titanium silicalite-1 catalytic films and application as catalytic membrane reactors, *Chem. Eng. J.* 156 (2010) 562–570.
- [51] S.M. Kwan, K.L. Yeung, Zeolite microfuel cell, *Chem. Commun.* (2008) 3631–3633.
- [52] W. Han, K.L. Yeung, Confined PFSA-zeolite composite membrane for self-humidifying fuel cell, *Chem. Commun.* 47 (2011) 8085–8087.